Arresting bubble coarsening: A model for stopping grain growth with interfacial elasticity

Anniina Salonen, Cyprien Gay, Armando Maestro, Wiebke Drenckhan, Emmanuelle Rio

Arresting bubble coarsening: A model for stopping grain growth with interfacial elasticity

Anniina Salonen,[1] Cyprien Gay,[2] Armando Maestro,[3] Wiebke Drenckhan,[1] and Emmanuelle Rio[1]

[1] *Univ Paris-Sud, Laboratoire de Physique des Solides, UMR8502, Orsay, F-91405*
[2] *Université Paris Diderot–Paris 7 Matière et Systèmes Complexes (CNRS UMR 7057), Bâtiment Condorcet, Case courrier 7056, 75205 Paris Cedex 13*
[3] *Univ Paris-Sud, Laboratoire de Physique des Solides, UMR8502, Orsay, F-91405*
Present address: Biological and Soft Systems, University of Cambridge, UK.

(Dated: May 6, 2015)

Many two-phase materials suffer from grain-growth due to the energy cost which is associated with the interface that separates both phases. While our understanding of the driving forces and the dynamics of grain growth in different materials is well advanced by now, current research efforts address the question of how this process may be slowed down, or, ideally, arrested. We use a model system of two bubbles to explore how the presence of an interfacial elasticity may interfere with the coarsening process and the final grain size distribution. Combining experiments and modelling in the analysis of the evolution of two bubbles, we show that clear relationships can be predicted between the interfacial tension, the interfacial elasticity and the change in bubble polydispersity. Despite its general interest, the presented results have direct implications for our understanding of foam stability.

Materials consisting of grains separated by well-defined interfaces are ubiquitous. Examples include polycrystalline solids [1], magnetic garnet films [2], two-phase ferrofluidic mixtures [3], superconducting magnetic froths [4], foams [5, 6] or emulsions [7]. In such systems, the positive energy associated with the interfaces is the driving force of a characteristic grain growth or "coarsening" process by which smaller grains tend to disappear while larger grains grow, leading to a progressive reduction of the overall interfacial energy and to characteristic asymptotic grain size distributions.

While our understanding of the main mechanisms of grain growth in these different systems has advanced significantly, much effort is now dedicated to the question of how this grain growth may be controlled or, ideally, completely arrested. Since the historic work by the metallurgist S. C. Smith [8], liquid foams have served repeatedly as model systems for related questions. We return here to this model system in order to tackle the question of how grain growth may be arrested by the presence of an interfacial elasticity E [9, 10], i.e. by interfaces whose interfacial tension γ depends on the interfacial area A, with a dilatational elastic modulus E defined as

$$E = \frac{\partial \gamma}{\partial \ln A}. \qquad (1)$$

In this context, a classical prediction for the growth arrest is due to Gibbs [9]. It consists in considering a single bubble of radius R and surface area $4\pi R^2$ in a liquid at constant pressure p_{liq}. In the absence of an interfacial elasticity, the gas pressure p_{gas} inside the bubble exceeds that in the liquid, the corresponding pressure drop being given by the Young-Laplace law $\Delta p = p_{\mathrm{gas}} - p_{\mathrm{liq}} = 2\gamma/R$. Since $\partial \Delta p/\partial R < 0$ this pressure drop increases with decreasing bubble size, leading to an accelerated bubble dissolution for a single bubble, and a net gas transport from smaller to bigger bubbles in multiple-bubble systems. Gibbs showed that this evolution can be not only slowed down but even fully arrested by the presence of a sufficiently high interfacial elasticity. Indeed, Eq. (1) implies that $\partial \Delta p/\partial R = \frac{2}{R^2}(2E - \gamma)$. Hence, when $E/\gamma > 1/2$, which is now known as the *Gibbs criterion* [9], the bubble evolution is stopped. This criterion

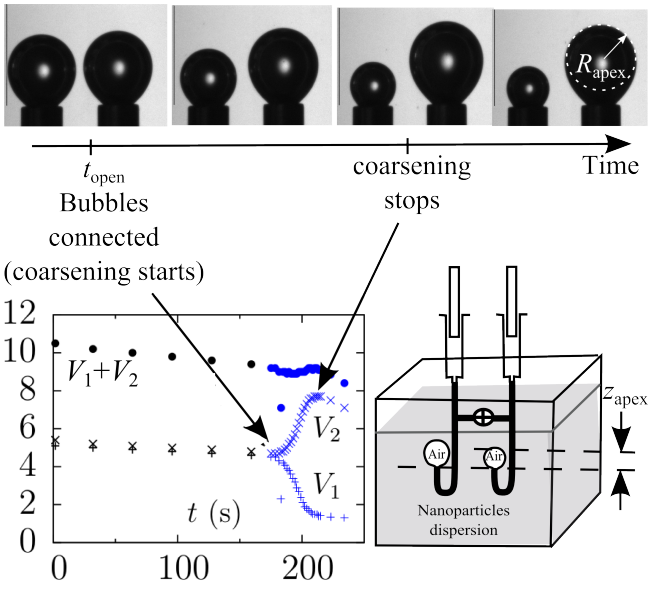

FIG. 1: Experimental set-up and bubble volume evolution. *Top:* photographs of the bubbles at four different times. *Bottom right:* setup. Two bubbles are prepared in a nanoparticle dispersion and left to equilibrate. A valve connects both bubbles. It is opened at t_{open}. Gas exchange between both bubbles occurs until they reach equal pressures. *Bottom left:* evolution of the bubble volumes (mm^3). The initial values correspond to a polydispersity factor $x_0 = 2.1\%$ while the final values correspond to $x_f = 0.69$.

has been checked by simulations more recently [10].

In the case of a single bubble, such an interfacial elasticity arises naturally when working with stabilising agents which are irreversibly adsorbed to the gas/liquid interface. Systems which are very much "en vogue" for this purpose consist of bubbles stabilised by nano- or micron-sized particles [11–13] or special proteins [14]. In this case, during the shrinking process, the agents are compacted at the interface, hence not only does the interfacial tension γ decrease, but the elastic modulus E itself increases. As a result, Gibbs' criterion $E/\gamma > 1/2$ is necessarily fulfilled at some point. However, many questions remain as to how the behaviour of a single bubble can be related to that of a complex foam which contains bubbles of different sizes – since some of them will shrink and others will grow. Many irreversibly adsorbed systems have proven to stop coarsening, with a surprisingly good agreement with the Gibbs criterion [14–18]. Nevertheless, it is not clear at this stage how to provide a reliable criterion for the coarsening to stop, and to predict the final bubble size distribution [10].

In order to provide a bridge between the one-bubble and the many-bubble systems, we here analyse theoretically and experimentally the coarsening process of a drastically simplified foam which consists of two bubbles which can exchange gas, as shown in FIG. 1. Using this simple system, we show that coarsening is expected to stop from the very beginning if the Gibbs criterion is fulfilled under the conditions *(i)* that the bubbles have exactly identical initial sizes, *(ii)* that there is no hydrostatic pressure difference between them and *(iii)* that there is no further adsorption onto the surface. If either of these three assumptions is relaxed, the Gibbs criterion evolves to higher critical values of the interfacial elasticity. We confirm this prediction by experiments performed on bubbles stabilised by nanoparticles.

The set-up we are interested in is schematised in FIG. 1. A small bubble (1) and a big bubble (2) are generated in a dispersion of nanoparticles made partially hydrophobic by the adsorption of oppositely charged surfactants. The two bubbles are connected by a tube. With spherical bubbles and neglecting any difference in hydrostatic pressure between the two bubbles, the pressure p_i in the bubble i writes:

$$p_i(t) \;=\; 2\gamma_i(t)/R_i(t) \tag{2}$$

Assuming that E does not depend on the surface area, Eq. (1) is valid over a wide range of surface areas, which yields an expression for the interfacial tension of each bubble:

$$\gamma_i(t) = \gamma_0 + E\ln(A_i(t)/A_{i,\mathrm{ini}}) \tag{3}$$

where $A_{i,\mathrm{ini}}$ is the initial area of the bubble i and $A_i(t)$ its evolution with time.

Let us now introduce the effective average radius R_0 and the polydispersity factor x through $2R_0^3 = R_1^3 + R_2^3$ and $2x = (R_2^3 - R_1^3)/R_0^3$, which yields:

$$R_1 \;=\; (1-x)^{1/3}\,R_0 \tag{4}$$

$$R_2 \;=\; (1+x)^{1/3}\,R_0 \tag{5}$$

where $x = 0$ if the bubbles have the exact same size while $x \to 1$ in the limit where the smaller bubble shrinks and disappears entirely. Using $A_i = 4\pi\,{R_i}^2$ and Eqs. (2), (3), (4) and (5), the pressure in each bubble can be written as:

$$p_1 \;=\; +\frac{2\gamma_0 + \frac{4}{3}E\ln\left(\frac{1-x}{1-x_0}\right)}{R_0\,(1-x)^{1/3}} \tag{6}$$

$$p_2 \;=\; +\frac{2\gamma_0 + \frac{4}{3}E\ln\left(\frac{1+x}{1+x_0}\right)}{R_0\,(1+x)^{1/3}} \tag{7}$$

At equilibrium, both pressures are equal, hence Eqs. (6) and (7) yield a prediction, in implicit form, for the final polydispersity x_f as a function of two control parameters, namely the initial polydispersity x_0 and the interfacial elasticity E:

$$\frac{2E}{3\gamma_0}\left[\frac{\ln\left(\frac{1-x_0}{1-x_f}\right)}{(1-x_f)^{1/3}} - \frac{\ln\left(\frac{1+x_0}{1+x_f}\right)}{(1+x_f)^{1/3}}\right] = \left[\frac{1}{(1-x_f)^{1/3}} - \frac{1}{(1+x_f)^{1/3}}\right] \tag{8}$$

As shown by FIG. 2a, Eq. (8) predicts that if the initial polydispersity x_0 is rigorously zero (black line), no coarsening occurs ($x_f = 0$) whenever $E/\gamma_0 \geq 1/2$, in other words Gibbs' criterion is strictly obeyed. Coarsening is expected as soon as $E/\gamma_0 \leq 1/2$ but it should stop after a finite change in bubble volume, i.e. for some final polydispersity x_f strictly between 0 and 1. If the initial bubbles have slightly different volumes ($x_0 > 0$), the criterion is less sharp (coloured lines in FIG. 2a). The larger the interfacial elasticity, the smaller is the final polydispersity x_f.

In order to test this prediction, we performed experiments on bubbles stabilized by a mixture of silica nanoparticles (ludox) and oppositely charged surfactants (CTAB) which is a well characterized system [19]. Two syringes are immersed in the solution and their outlets are positioned at the same altitude. A bubble is generated at the outlet of each syringe by pressing them manually (FIG. 1). Both syringe outlets are connected by a tube which is initially closed by a valve. Both bubbles are left to equilibrate separately, then at $t_{\mathrm{open}} = 170$s, the valve is opened and the gas is free to flow from one bubble to the other. The bubble evolution is recorded with a video camera. The pictures are then treated by the software included in a Tracker (Teclis, France) to extract the volume, radius, interfacial tension, apex altitude and apex radius of curvature of each bubble as a function of time.

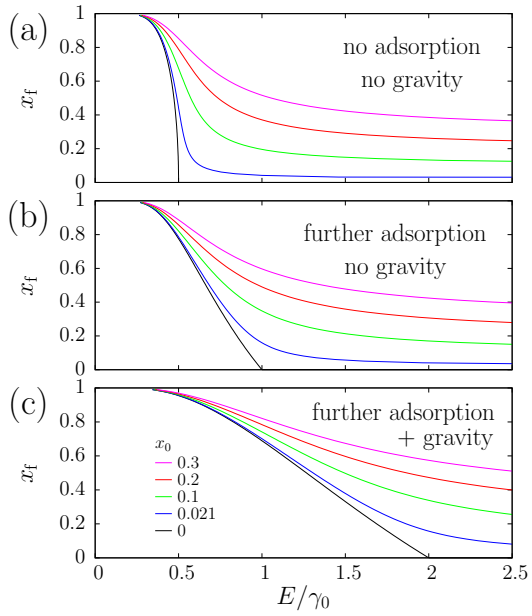

FIG. 2: Expected effect of elasticity, adsorption and gravity on the final bubble volumes for irreversibly adsorbed surfactants according to: (a) Eq. (8), (b) Eq. (10) and (c) Eq. (12). The final volume of the big (resp. small) bubble is proportional to $1 + x_f$ (resp. $1 - x_f$). Further adsorption onto the big (growing) bubble is assumed to be blocked in (a). It is present in (b) and (c). The effect of gravity on the pressure is neglected in (a) and (b). In (c), gravity is taken into account and the ratio of the average bubble radius R_0 to the capillary length $\ell_{\rm cap} = \sqrt{\gamma_0/(\rho g)}$ is taken equal to 1.0. Black curves correspond to initially identical bubbles (initial polydispersity factor $x_0 = 0$) while coloured curves correspond to $x_0 = 2.1\%$ (experimental value), 10%, 20% and 30%.

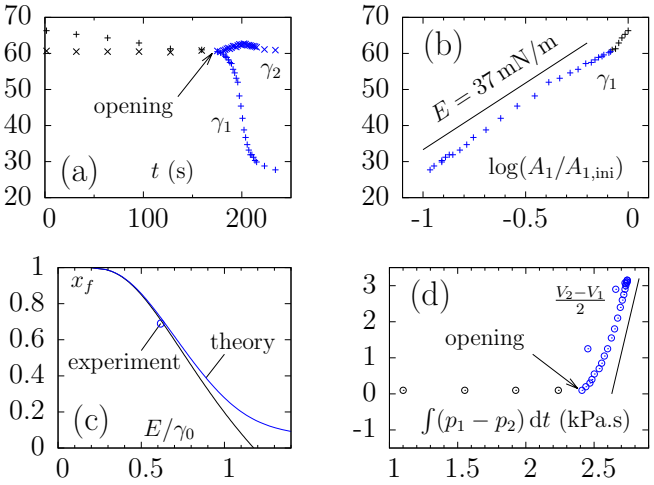

FIG. 3: Measured bubble evolution while the bubbles are isolated (black data points, $t < t_{\rm open} = 170$s) and once they have been connected (blue points, $t > t_{\rm open}$). *(a)* Interfacial tensions (mN/m) extracted from bubble shapes and sizes. The initial value at $t_{\rm open}$ is $\gamma_0 = 60$mN/m. *(b)* Interfacial tension γ_1 of the small bubble as a function of the logarithm of its surface area A_1. The straight line, as a guide for the eye, corresponds to an estimated elasticity $E = 37\,$mN/m. *(c)* Theoretical prediction for $x_0 = 2.1\%$, $E/\gamma_0 = 0.62$ and $R_0/\ell_{\rm cap} = 0.42$ (blue line), and comparison with the experimental value (blue circle). The case of two initially stricly identical bubbles ($x_0 = 0$) is shown for comparison (black curve). *(d)* Cumulated gas flow (mm^3) between both bubbles (*i.e.*, volume of the gas transferred) as a function of the cumulated pressure difference as derived from the bubble dimensions *via* Eq. (14). The slope reaches a final value which corresponds to the hydrodynamic conductance of the connection between both bubbles.

FIG. 1 displays the evolution of the volume V_1 and V_2 of the big and the small bubble respectively. After the bubbles are connected at $t_{\rm open}$, the smaller bubble shrinks while the bigger one grows. This coarsening behaviour stops after a while and the bubbles reach a rather stable final volume. This corresponds qualitatively to the predicted behavior represented in FIG. 2(a). Note that the total volume decreases slowly with time (see FIG. 1). This indicates a small dissolution of the bubbles into the bath.

For a quantitative comparison, the evolution of the measured interfacial tensions, initially identical, are plotted in FIG. 3a. The interfacial tension γ_1 of the smaller bubble decreases with time and the elasticity is almost constant ($E = 37\,$mN/m, see FIG. 3b), which justifies the use of Eq. (3). Thus, the small bubble can be described using the above assumption that no desorption occurs during shrinking. By contrast, the interfacial tension of the bigger bubble is almost constant during the experiment (FIG. 3a), which suggests that adsorption takes place on much shorter timescales than those of the experiment. In other words, there is an asymmetry between the big bubble (fast adsorption) and the small one (no desorption).

Let us now therefore complement the model with the effect of particle adsorption, which we assume instantaneous, when bubble 2 grows. The fast adsorption results in a constant surface coverage and interfacial tension:

$$\gamma_2(t) = \gamma_0 \tag{9}$$

Under such circumstances, Eq. (8) is modified and the condition $p_1 = p_2$ now reads:

$$\frac{2E}{3\gamma_0}\,\frac{\ln\left(\frac{1-x_0}{1-x_f}\right)}{(1-x_f)^{1/3}} = \left[\frac{1}{(1-x_f)^{1/3}} - \frac{1}{(1+x_f)^{1/3}}\right] \tag{10}$$

This modifies the prediction for the final volume of the two bubbles (FIG. 2b). The result is qualitatively the same. However *(i)* the Gibbs criterion becomes $E/\gamma_0 > 1$ for $x_0 = 0$ and *(ii)* for $E/\gamma_0 < 1$, the final polydispersity factor x_f increases less sharply with a decreasing interfacial elasticity.

Let us now incorporate another feature into the model, namely the effect of gravity. In the experiment, the syringe outlets are positioned at the same altitude. As a

consequence, the apex of the big bubble is higher than that of the small one, which reinforces the pressure difference between them and accelerates the coarsening process. To take this effect into account, we complement Eq. (2) with the hydrostatic pressure:

$$p_i(t) \;=\; 2\gamma_i(t)/R_i(t) - 2\rho g R_i(t) \qquad (11)$$

Defining the capillary length $\ell_{\rm cap} = \sqrt{\gamma_0/(\rho g)}$, this yields:

$$\frac{2E}{3\gamma_0}\frac{\ln\left(\frac{1-x_0}{1-x_f}\right)}{(1-x_f)^{\frac{1}{3}}} \;=\; \left[\frac{1}{(1-x_f)^{\frac{1}{3}}} - \frac{1}{(1+x_f)^{\frac{1}{3}}}\right] + \frac{R_0^2}{\ell_{\rm cap}^2}\left[(1+x_f)^{\frac{1}{3}} - (1-x_f)^{\frac{1}{3}}\right] \qquad (12)$$

The prediction for the final volume for $R_0 = \ell_{\rm cap}$ is plotted in FIG. 2c for various initial polydispersities x_0. As can be seen from the (black) curve, for $x_0 = 0$, Gibbs' criterion turns out to become: $E/\gamma_0 > 2$, which indicates that the two-bubble system is more strongly destabilized than when gravity was not taken into account (compare with FIG. 2b). Eq. (12) shows that this effect will be stronger when the bubble size R_0 is larger. More generally, taking Eq. (12) with $x_0 = 0$ and taking the limit $x_f \to 0$, we obtain the new version of Gibbs criterion:

$$\frac{E}{\gamma_0} = k_{\rm ads}\left(1 + \frac{R_0^2}{\ell_{\rm cap}^2}\right) \qquad (13)$$

where $k_{\rm ads} = 1/2$ when no adsorption takes place, as in Eq. (8), and $k_{\rm ads} = 1$ for fast adsorption as in Eqs. (10-12).

Let us now draw a quantitative comparison between the prediction provided by the full model, given by Eq. (12), and the experiment. The initial bubble volumes, 4.4 and 4.6 mm^3, (see FIG. 1) correspond to a polydispersity factor $x_0 = 0.021$ while the final volumes, 1.3 and 7.1 mm^3, correspond to $x_f = 0.69$. The value of the effective average radius $R_0 = 1.0$ mm results from the initial average volume $4\pi R_0^3/3 = 4.5$ mm^3. The initial surface tension $\gamma_0 = 60$ mN/m (see FIG. 3a) yields the capillary length $\ell_{\rm cap} = 2.45$ mm, *i.e.*, $R_0/\ell_{\rm cap} = 0.42$. Finally, the elasticity $E = 37$ mN/m (see FIG. 3b) yields the value of the ratio $E/\gamma_0 = 0.62$. These values can now be used to plot the prediction that corresponds to the values of x_0 and $R_0/\ell_{\rm cap}$. It agrees remarkably well with the experimental value of E/γ_0 and x_f, see FIG. 3c.

Let us now check whether the above theoretical description, successful for predicting the final state, can also account for the time evolution within our experiment. If the gas flowrate between both bubbles is proportional to the difference in pressure, then the volume $(V_2 - V_1)/2$ transfered from bubble 1 to bubble 2 should vary like the integral of the pressure difference, $\int_0^t (p_1 - p_2)dt$. Let us estimate the pressures p_i using a modified version of Eq. (11) to take into account a more realistic (not necessarily spherical) bubble shape:

$$p_i(t) \;=\; 2\gamma_i(t)/R_i^{\rm apex}(t) - \rho g z_i^{\rm apex}(t), \qquad (14)$$

where the apex altitude $z_i^{\rm apex}$, the radius of curvature $R_i^{\rm apex}$ at the apex and the interfacial tension γ_i can be extracted from the pictures at all time. The result is shown on FIG. 3d. The linear variation that is reached eventually (*i.e.*, when the flowrate is low according to FIG. 1) shows that Eq. (14) is valid, as expected. In principle, it should also be used in the theory, rather than Eq. (11), especially for initial bubble radii R_0 comparable to the capillary length $\ell_{\rm cap}$. This can be done only numerically, however, and we believe that the essential trends are already captured by the present spherical-bubble version of the theory.

This comparison between a model and a simple experiment performed on two interconnected bubbles allows to rationalize why the Gibbs criterion describes foams qualitatively well even if the threshold of 1/2 is not always recovered experimentally. We indeed show in this Letter that the Gibbs criterion describes well the case of two bubbles stabilized by agents which are all irreversibly adsorbed to the interface from the beginning, in the absence of gravity, *i.e.*, for small bubbles, and for initially monodisperse bubbles. In this case, the coarsening does not even start if $E/\gamma_0 > 1/2$. If the bubbles are initially polydisperse, the criterion is somewhat relaxed: the coarsening starts, but it stops before the small bubble can disappear. In the presence of gravity or in the presence of fast adsorption, the classical threshold value 1/2 for the Gibbs criterion increases and the total arrest of the coarsening is predicted by a new version of Gibbs criterion, given by Eq. (13). We have shown that when all these different effects are taken into account, the experiments are well captured by the theoretical description. Coarsening indeed stops experimentally after a finite time and bubbles reach a finite volume.

In order to generalize the present study and describe foam coarsening completely, additional steps still need to be taken because it may differ from the present two-bubble situation for at least three reasons: *(i)* when a given bubble swells or shrinks, its various films may change size at different rates, depending on the dynamics of the neighbouring bubbles, *(ii)* different bubbles in a foam have different altitudes, hence the intensity and the sign of the gravity term in Eq. (13) depend on the pair of bubbles under consideration, and *(iii)* in a dry foam, the pressure in the liquid, located in the films and in the channels (called Plateau borders) between neighbouring bubbles, is significantly lower than the gas pressure in the bubbles themselves. More generally, the fact that the coarsening behaviour of two bubbles is very different from that of a single bubble, as we have shown, suggests that coarsening in 3D foams may reflect complex collective behaviours.

We believe that the physical understanding we have gained from the two-bubble system can be translated directly to other systems which undergo grain growth. Most realistic systems are likely to have a more complex elastic behaviour than the one considered here. Al-

ready in the case of bubbles one may think about more complex scenarios, for example when considering soluble surfactants with slow desorption/adsorption. In this case, the coarsening would not be stopped, but the overall coarsening dynamics would be affected. Last but not least, many systems which undergo grain growth consist of polyhedral grains in which the grain pressure is correlated with the grain size *via* the grain topology - *i.e.* in a less direct manner than considered here for spherical bubbles.

We would like to acknowledge fruitful discussions with I. Cantat and D. Langevin. A. Maestro is grateful to the CNRS for financing his position. We acknowledge funding from the European Research Council (ERC Starting Grant 307280-POMCAPS).

[1] V. Novikov. *Grain Growth and Control of Microstructure and Texture in Polycrystalline Materials*. CRC Press, 1996.

[2] D. Weaire, F. Bolton, P. Molho, and J. A. Glaziers. Investigation of an elementary model for magnetic froth. *Journal of Physics: Condensed Matter*, 3(13):2101, 1991.

[3] F. Elias, C. Flament, J. C. Bacri, O. Cardoso, and F. Graner. Two-dimensional magnetic liquid froth: Coarsening and topological correlations. *Physical Review E*, 56(3):3310–3318, 1997.

[4] R. Prozorov, A. F. Fidler, J. R. Hoberg, and P. C. Canfield. Suprafroth in type-i superconductors. *Nature Physics*, 4(4):327–332, 2008.

[5] D. Weaire and S. Hutzler. *The Physics of Foams*. Clarendon Press, Oxford, 1999.

[6] I. Cantat, S. Cohen-Addad, F. Elias, F. Graner, R. Hohler, O. Pitois, F. Rouyer, and A. Saint-Jalmes. *Foams - Structure and Dynamics*. Oxford University Press, Oxford, UK, 2013.

[7] B. P. Binks. *Modern aspects of emulsion science*. Royal Society of Chemistry, 1998.

[8] C. S. Smith. *A search for structure : selected essays on science, art and history*. MIT Press, Cambridge, Mass., 1981.

[9] J. W. Gibbs. *The scientific papers of J. Willard Gibbs*. Oxbow press, Woodridge, 1993.

[10] William Kloek, Ton van Vliet, and Marcel Meinders. Effect of bulk and interfacial rheological properties on bubble dissolution. *Journal of Colloid and Interface Science*, 237(2):158–166, 2001.

[11] Urs T. Gonzenbach, André R. Studart, Elena Tervoort, and Ludwig J. Gauckler. Stabilization of foams with inorganic colloidal particles. *Langmuir*, 22(26):10983–10988, 2006.

[12] Tommy S. Horozov. Foams and foam films stabilised by solid particles. *Current Opinion in Colloid & Interface Science*, 13(3):134–140, 2008.

[13] Eric Dickinson. Food emulsions and foams: Stabilization by particles. *Current Opinion in Colloid & Interface Science*, 15(1–2):40–49, 2010.

[14] T. B. J. Blijdenstein, P. W. N. de Groot, and S. D. Stoyanov. On the link between foam coarsening and surface rheology: why hydrophobins are so different. *Soft Matter*, 6(8):1799–1808, 2010.

[15] A. Cervantes Martinez, E. Rio, G. Delon, A. Saint-Jalmes, D. Langevin, and B. P. Binks. On the origin of the remarkable stability of aqueous foams stabilised by nanoparticles: link with microscopic surface properties. *Soft Matter*, 4(7):1531–1535, 2008.

[16] Antonio Stocco, Wiebke Drenckhan, Emanuelle Rio, Dominique Langevin, and Bernard P. Binks. Particle-stabilised foams: an interfacial study. *Soft Matter*, 5(11):2215–2222, 2009.

[17] Daniela Georgieva, Alain Cagna, and Dominique Langevin. Link between surface elasticity and foam stability. *Soft Matter*, 5(10):2063–2071, 2009.

[18] Andrew R. Cox, Deborah L. Aldred, and Andrew B. Russell. Exceptional stability of food foams using class ii hydrophobin hfbii. *Food Hydrocolloids*, 23(2):366–376, 2009.

[19] Armando Maestro, Emmanuelle Rio, Wiebke Drenckhan, Dominique Langevin, and Anniina Salonen. Foams stabilised by mixtures of nanoparticles and oppositely charged surfactants: relationship between bubble shrinkage and foam coarsening. *Soft Matter*, 10(36):6975–6983, 2014.